The self-excitation damping ratio:

A chatter criterion for time-domain milling

simulations

Neil D Sims, MIMechE

Advanced Manufacturing Research Centre with Boeing,

Department of Mechanical Engineering, The University of Sheffield,

Mappin St, Sheffield S1 3JD, UK

Email: n.sims@sheffield.ac.uk

Phone: +44 114 2227724

Fax: +44 114 2227890

33 pages including 11 Figures.

Abstract

Regenerative chatter is known to be a key factor that limits the productivity of high speed machining. Consequently, a great deal of research has focussed on developing predictive models of milling dynamics, to aid engineers involved in both research and manufacturing practice. Time-domain models suffer from being computationally intensive, particularly when they are used to predict the boundary of chatter stability, when a large number of simulation runs are required under different milling conditions. Furthermore, to identify the boundary of stability each simulation must run for sufficient time for the chatter effect to manifest itself in the numerical data, and this is a major contributor to the inefficiency of the chatter prediction process.

In the present article, a new chatter criterion is proposed for time-domain milling simulations, that aims to overcome this drawback by considering the transient response of the modelled behaviour, rather than the steady-state response. Using a series of numerical investigations, it is shown that in many cases the new criterion can enable the numerical prediction to be computed more than five times faster than was previously possible. In addition, the analysis yields greater detail concerning the nature of the chatter vibrations, and the degree of stability that is observed.

Nomenclature

b	Depth of cut
dz	Thickness of elemental layer
f	Analysis frame
F	Number of analysis frames
$F_{r,p,l}$	Radial forces for tooth p and axial layer l
$F_{t,p,l}$	Tangential forces for tooth p and axial layer l
$h_{p,l}$	Instantaneous chip thickness for tooth p layer l
k	Spectral index
k_p	Spectral indices which have a local maxima in the magnitude of the Fourier series
$k_{p,max}$	Spectral index corresponding to the least stable self-excitation frequency
K_{rc}	Radial cutting stiffness coefficient
K_{tc}	Tangential cutting stiffness coefficient
m	Harmonic number
N	Number of simulation time steps per tool revolution
n_t	Number of teeth on the tool
Sa_p	Surface coordinate array (complex Cartesian notation) for tooth p
x	Discrete vibration signal
X	Fourier series of x
x_1, x_2	Successive vibration oscillations of a freely decaying structure
X_{se}	Self-excitation terms in the Fourier series X
δ	Logarithmic decrement
$\delta_{r,kp}$	Logarithmic decay per revolution for spectral index k_p
$\delta_{r,kpmax}$	Logarithmic decay per revolution for spectral index k_{pmax}
η	Ratio of the maximum chip thickness predicted with and without structural vibration
ζ	Damping ratio

Introduction

The productivity of high speed milling operations is limited by the onset of regenerative chatter. This occurs when relative vibrations between the cutting tool and workpiece modulate the cutting force, leading to a self-excited vibration. Depending on cutting conditions such as the spindle speed and depth of cut, the self-excited vibration can either decay (producing a stable cut), or grow in an unstable fashion to result in chatter. This causes an unacceptable surface finish, along with excessive tool wear or breakage, thereby limiting the metal removal rate that can be achieved.

There has been a great deal of work to investigate the phenomenon of regenerative chatter, and to develop efficient methods for chatter prediction and avoidance. Chatter prediction techniques combine models of the cutting forces with models of the machine system dynamics, to predict the vibrational behaviour of the system. The pioneering work by Tlusty [1] and Tobias [2] developed analytical, or frequency domain predictions of chatter in turning. More recently, similar approaches have been used to predict chatter in milling [3, 4]. These analytical approaches have the advantage of being relatively fast to compute, but they usually involve a number of simplifications and assumptions regarding the mechanics of the milling process, which reduces the accuracy of the predictions. An alternative approach is to predict the onset of chatter using time-domain simulations of the milling process. This allows more complex nonlinear models of the cutting forces and system dynamics, so that the accuracy of the chatter prediction is enhanced. Time domain solutions tend to be computationally intensive, requiring a large number of simulation permutations under different cutting conditions in order to find the boundary of chatter stability.

The problem also arises of how to ascertain, based upon the computed data, whether the simulated cut was stable or unstable. A chatter detection criterion is required, a number of which have been proposed in the literature. The peak-to-peak (PTP) forces method was proposed by Smith and Tlusty [5], who showed that as the cutting conditions approach the boundary of stability, the PTP forces increase dramatically, enabling a graphical visualisation of the stability boundary. Campomanes and Altintas [6] suggested that this approach was less accurate for low radial-immersion cutting, and proposed a non-dimensional chatter coefficient based upon the predicted chip thickness. In their

method, the maximum chip thickness that occurs during a simulation with the flexible machine system is compared to that obtained using a rigid system (i.e. where chatter cannot occur). A similar approach was suggested by Li *et al* [7], who based their coefficient on the resulting forces, rather than the chip thickness. Bayly *et al* [8] used an alternative approach that applied signal processing techniques to the simulated tool displacement data. They sampled the data once per tooth revolution and calculated the statistical variance of the signal: a large variance has been shown to be a good indicator of chatter [9].

It is interesting to note that a chatter detection criterion is also required when investigating milling chatter experimentally, rather than in simulations. In this case, spectral analysis of audio measurements is well-known to be a good approach [10]. However, in experimental tests it is easy to generate long sequences of measurement data (representing hundreds or thousands of revolutions of the tool), giving a high resolution in the frequency domain. In contrast, the computational effort required in simulations means that it is desirable to detect chatter after as few revolutions of the tool as possible, thereby reducing the simulation time.

With this issue in mind, the present study proposes an alternative approach to detecting chatter in time-domain milling simulations. Unlike the methods previously described [5, 6, 8], the proposed technique is directly related to concepts of feedback stability and damping (so it is more physically meaningful) and requires substantially shorter simulation runs. The remainder of this contribution is organised as follows. First, the proposed chatter criterion is introduced from a vibrations perspective, before describing the key aspects of a time domain model that is based upon that developed by Campomanes and Altintas [6]. Next, numerical results are presented in the form of four case studies which investigate the performance of the criterion under various conditions. It should be noted at this stage that although no experimental data is included, the results will be compared with previously validated [6] and commercially available software [13]. Finally, the results are discussed and some conclusions are drawn.

Chatter criterion

In vibrations theory, it is well known that when viscously damped structures are allowed to freely vibrate, they exhibit a form of vibration decay as shown in Figure 1. It can be shown [11] that for low levels of damping, the damping ratio, ζ, is related to the amplitude of two successive oscillations, x_1 and x_2, by:

$$\zeta = \frac{\delta}{2\pi}; \qquad \delta = \log\frac{x_1}{x_2} \qquad \textbf{(1)}$$

The so-called logarithmic decrement, δ, is therefore a useful tool for vibration testing since it gives an immediate indication of the level of damping and can be determined from just a few measured vibration cycles.

Linear self-excited vibrations can be thought of in the same fashion, but if the self-excited system is nonlinear, or non-viscously damped, then the way in which the vibration amplitudes grow (or decay) will be different. For example, hysteretically damped systems will exhibit a linear decay in the free-vibration amplitude [11], so the same behaviour is expected for the corresponding self-excited system.

The question that arises here is whether a concept similar to the logarithmic decrement can be developed as a measure of chatter stability. In principle, this would require just a few cycles of the self-excited vibrations in order to characterise the chatter stability. Consequently, the time-domain model need only run for a few simulated cycles of the tool, substantially reducing the computational effort. Furthermore, the approach would offer more physical insight into the chatter stability, based directly upon concepts of damping and stability.

However, there are two issues that must be overcome: the vibrations observed in milling simulations are dominated by the forced vibrations due to the tool rotation, and the self-excitations that give rise to chatter may be nonlinear and not necessarily viscously damped. The former can be avoided by a suitable signal processing technique, whereas the latter will be addressed in a numerical study. However, before tackling these issues, a time-domain milling model will be described that can be used in conjunction with the chatter criterion.

Time domain milling model

A number of milling time-domain models have been proposed in the literature [6, 7, 12], some of which are now commercially available [13, 14]. In the present study, the model proposed by Campomanes and Altintas [6] will be used with some simplifications. It should be noted that the aim here is not to create a new model of milling, but to develop a new technique for analysing the model results, in terms of chatter stability. Consequently, the model is only briefly summarised here; for a more complete description, the interested reader is referred to [6].

The model used in the present study consists of three aspects, namely milling kinematics, milling forces, and system dynamics. The kinematics model begins by dividing the tool into discrete axial slices, and calculating the tool and workpiece geometry within each slice. Two coordinate systems are used: a radial coordinate based upon the centre of the tool with angles taken relative to the feed direction, and a Cartesian coordinate system based upon the workpiece feed direction. The relative displacement of the workpiece and tool (accounting for feed rate and vibration effects) are provided as inputs to the calculation. The basis of the computation is the manipulation of a set of arrays of Cartesian coordinates (one array for each tooth on each axial slice), that define the surface of the workpiece that was produced by that tooth. The array length represents a complete revolution of the tooth, therefore with each tooth revolution the array values are overwritten, or updated. For each time step in the simulation, the following calculations are repeated for each tooth on each axial slice:

1) The position of the tooth is calculated based upon the current simulation time, and the spindle speed.

2) The workpiece surface array for the present tooth is updated,

3) The instantaneous chip thickness for the present tooth is calculated, based upon the current tooth position, and the surface array for the preceding tooth.

The process is illustrated by the example shown in Figure 2a, which shows one discrete axial slice of the tool along with the corresponding teeth positions, and the discrete surface arrays. The close-up shown in Figure 2b demonstrates how the surface array for the current tooth (Sa_p) is updated based

upon the position of the tooth. Figure 2c shows how the corresponding chip thickness is calculated based upon the tooth position and the surface array generated by the preceding tool, Sa_{p-1}. However, during milling the tooth can lose contact with the surface, either because it has rotated outside of the cut, or because of the vibrations between the tool and workpiece. The latter case is illustrated in Figure 3, where the tooth tip does not intersect the surface array generated by the preceding tooth (Sa_{p-1}). In this case, the surface array for the tooth (Sa_p) is updated by interpolation between the data points of Sa_{p-1}. In physical terms, this is equivalent to the workpiece surface being unchanged, since the tooth is not cutting. In this situation, the instantaneous chip thickness is zero.

The milling forces computation takes the instantaneous chip thicknesses that have been calculated for each tooth p and axial slice l of the kinematics computation. The corresponding cutting forces are determined as a radial component $dF_{r,p,l}$ (into the tool centre) and a tangential component $dF_{t,p,l}$ opposing the rotation of the tool:

$$
\begin{aligned}
F_{r,p,l} &= K_{rc}\, h_{p,l}\, dz \\
F_{t,p,l} &= K_{tc}\, h_{p,l}\, dz
\end{aligned}
\tag{2}
$$

Here, K_{rc} and K_{tc} are cutting stiffness coefficients that are experimentally determined, and dz is the thickness of each axial slice. The forces are then transformed into the workpiece Cartesian coordinates, and numerically integrated to give the resultant cutting forces in the x and y directions.

Finally, the system dynamics are modelled as state-space formulations of modal models that represent the behaviour of the tool in the x and y directions. At the next simulation step, these displacements (along with the feed-rate) are used to update the relative position of the tool and workpiece. In the present study, the computations were performed using a combination of Simulink [15] and a c-program that computed the milling kinematics. The Simulink block diagram is shown in Figure 4 which demonstrates the relationship between the cutting process and system dynamics. This modelling approach allows for rapid analysis of the simulation data using Matlab.

In comparison with the more advanced model described by Campomanes and Altintas [6], the present model has the following simplifications:

- The system dynamics are assumed to be the same for all the axial slices of the tool. Consequently, the bending-type mode-shapes of the tool are not modelled as accurately,

- Only 'arc surface arrays' were used, whereas reference [6] included workpiece lower and upper surface arrays to improve accuracy and efficiency in low-radial-immersion milling,

- Edge forces were neglected in the cutting force model, reducing the accuracy in low-radial-immersion milling.

Despite these simplifications, the model serves its purpose of generating reasonably accurate simulation data to which the proposed stability criterion can be applied. In the next section, this stability criterion will be described.

Signal processing method

In milling simulations, the self-excited vibrations that cause chatter are not clearly evident, since the forced vibrations (due to the rotation of the tool) dominate the response of the system. This is particularly the case in the region of marginal chatter instability, where the self-excited vibrations will grow very slowly. Consequently, many chatter criteria require the simulation to run for a long period of time before it is possible to determine if the system is stable or unstable.

An alternative approach is to isolate the self-excited vibrations from the forced vibrations, using Fourier analysis. This method is widely used in milling experiments [10] and simulations, to investigate the *steady-state* response of the cutting process in stable and unstable cutting. In what follows, the Fourier analysis will be extended to consider the *transient* response of the system, thereby allowing calculation of the damping ratio of the system before it reaches steady state. The method will therefore be referred to as the 'self-excitation damping ratio' chatter criterion. It should be noted that in their chatter criterion for turning operations, Kondo *et al* [16] also considered the transient behaviour. However, they defined the transient vibrations based upon the transfer function estimate of successive surface modulations, making the approach unsuitable for the milling process, which includes forced vibrations.

The analysis technique used in the present study is shown schematically in Figure 5. With reference to this figure, the first step is a time-domain simulation of the cutting process under given parameters (e.g. spindle speed, depth of cut, and cutting geometry). This leads to predicted vibration data for each degree of freedom of the system (e.g. tool vibration and workpiece vibration in the x and y directions). It is important that these signals are recorded at a sample rate which is an integer multiple N of the spindle rotational frequency. A Fourier analysis approach is then applied to each of these data sets, as follows:

First, the discrete signal x is divided into F frames to give $x(n,f)$, with the data $n=1,2,…,N$ in each frame f representing one complete revolution of the milling tool ('B' in Figure 5). The discrete Fourier transform is then obtained ('C' in Figure 5), which is given by:

$$X(k,f) = \sum_{n=1}^{N} x(n,f) \times e^{\frac{-2\pi j (k-1)(n-1)}{N}} \qquad 1 < k < N; \quad 1 < f < F \qquad \textbf{(3)}$$

This transform consists of a sequence of complex numbers, each describing the magnitude and phase of the vibration at frequencies which are precise fractions of the tool rotational frequency Ω. The first value ($k=1$) in the sequence corresponds to zero-frequency content of the vibration signal, 0Ω, the second value ($k=2$) corresponds to sinusoidal vibrations that have one cycle per rotation of the tool, 1Ω, the third corresponds to vibrations at twice the tool rotation frequency, 2Ω, and so on up to the Nyquist frequency $N\Omega/2$. Having carefully selected the sampling frequency of the vibration data in this way, the frequencies of the forced vibrations will all lie on the 'spectral lines' of the Fourier transform, given by:

$$k = m + n_t \qquad \textbf{(4)}$$

where m is an integer greater than zero that represents the harmonic number and n_t is the number of teeth on the tool. In other words, there is no spectral leakage of the forced vibrations, so they do not contaminate other regions of the Fourier transform. This remains the case provided the tool has a uniform pitch. The spectral lines with indices given by (4) can be ignored ('D' on Figure 5), by setting their values to zero, so that the Fourier transform only contains information on the self-excited vibrations:

$$X_{se}(k,f) = X(k,f); \quad X_{se}(m+n_t,f) = 0$$
$$\text{where} \quad 1 < k < N/2; \ m = 1,2,3,...,N/2-n_t; \ 1 < f < F \quad \textbf{(5)}$$

Equation (5) has also truncated the Fourier series at the index N/2, corresponding to the Nyquist frequency. This data can be studied as the frame number f increases, to see whether the vibrations at each frequency grow or decay. In practice, a large number of the spectral lines have only low magnitude, and so they can be ignored ('E' on Figure 5). This can be achieved by selecting the spectral lines $X_{se}(k_p,f)$ that have a maximum for one of the frames of data. These lines can then be plotted on a natural-logarithmic scale, thereby indicating the vibration decay per revolution of the tool ('F' on Figure 5).

The gradient of a straight line fit to the data can indicate the logarithmic decay per tool revolution, $\delta_{R,kp}$, corresponding to the spectral index k_p The index that corresponds to the steepest gradient is then referred to as $k_{p,max}$. The logarithmic decay per revolution, $\delta_{R,kpmax}$ describes the least stable self-excited oscillations. However, there will be a number of these oscillations of per revolution of the tool, so the value of $\delta_{R,kpmax}$ does not equal the logarithmic decrement per vibration cycle. The Fourier transform operation has averaged the magnitude of these oscillations within each frame. The number of self-excited oscillations per tool revolution is given by the index number $k_{p,max}$, so that the damping ratio ζ can be estimated by:

$$\zeta = \delta_{R,kpmax}/(2k_{p,max}\pi) \quad \textbf{(6)}$$

The accuracy of this damping ratio estimate is diminished by a rounding error, since the spectral index $k_{p,max}$ is an integer value whereas there will not be an integer number of self-excited vibrations per tool revolution. However, this does not affect the boundary of stability, where $\zeta=0$ and $\delta_{R,kpmax}=0$.

Although this signal processing approach appears somewhat protracted, it is relatively straightforward to implement. For example, using Matlab, the computations involve less than 30 lines of code and compute in under 0.1 seconds. In the next sections, a selection of numerical examples will be used to demonstrate the performance of the technique.

Case study 1: Single degree-of-freedom system

To begin, a simple milling scenario is considered, with one degree of freedom, to illustrate the effect of the depth of cut on the self-excitation damping ratio, ζ. Full details of the simulation parameters are given in Table 1.

Figure 6 serves to illustrate the steps of the signal processing method. Figure 6(A) illustrates the predicted tool chip thickness, and Figure 6(B) shows the corresponding vibration data for the tool in the y-direction. These steps correspond to 'A' and 'B' on Figure 5, respectively. The signals have been divided into 10 non-overlapping frames, one for each cycle of the tool (which has 4 teeth). Figure 6(C) shows the magnitudes of the discrete Fourier transform of the vibration signal, which contains both self-excited and forced-vibrations. In Figure 6(D), the spectral lines corresponding to the forced-vibrations are removed. Now, the decay in the self-excited vibration is clearly evident. This result is emphasised in Figure 6(E), where each spectral line is plotted against the frame number. One spectral line dominates the data, and taking natural logarithms gives the graph shown in Figure 6(F). Notice that the first data point appears to be spurious, but in fact this data corresponds to the first frame of the data, or first rotation of the tool. Referring to Figure 6(A), it can be seen that the tool is only just starting to engage in the cut during this frame. Consequently, this data point can be ignored. The linearity of the data in Figure 6(F) therefore demonstrates that the self-excited vibrations decay in a viscous fashion.

For the same spindle speed, the depth of cut was now changed incrementally, and the chatter analysis performed for each case. Figure 7 shows the results of the chatter analysis (Figure 7a) along with the chip thickness for the last simulated revolution of the tool (Figure 7b). In this case, the analysis frames have been overlapped so as to increase the number of data points available. For the 10mm cut, the self-excited vibrations are seen to be decaying with each rotation of the tool, giving a positive (i.e. stable) damping ratio of 0.0016. By the time of the last tool revolution, the vibrations have decayed to the extent that they are barely discernable on the chip thickness plot (Figure 7b). For the 12mm depth cut, the vibration decays less rapidly, with a damping ratio of 0.0004. The self-excited vibrations can now be observed on the chip thickness plot for the last revolution of the tool.

Increasing the depth of cut to 14mm results in chatter instability. The self-excited vibrations now grow with each cycle, as shown in Figure 7a. Despite the chatter, the vibration still exhibits an exponential growth as would be the case for a negative-viscously damped system. The calculated damping ratio for this case is -0.001, and the self-excited vibrations are clearly observed on the chip thickness plot. Increasing the depth of cut to 16mm causes the instability to worsen – the vibrations grow exponentially at a higher rate, giving $\zeta=0.002$. However, towards the final few revolutions the vibrations stop growing exponentially, so the data on Figure 7a is no longer linear. This can be explained with reference to Figure 7b, which shows how the teeth are starting to lose contact with the workpiece during the cut, thereby increasing the nonlinearity of the system. This phenomenon is more pronounced for 18mm depth of cut. Here, the loss of contact has caused the self-excited vibrations to stabilise after about 10 revolutions of the tool. Consequently, the calculated damping ratio is similar to that for the 16mm depth cut.

To recap, it appears that the self-excitation damping ratio provides an elegant method of analysing the chatter stability, despite the nonlinearity of the system. In contrast to other chatter criteria, the convergence of the solution does not depend upon the simulation reaching a steady-state condition. This is particularly valuable, since by definition vibrations near the boundary of stability will either grow or decay very slowly, so that the system takes an inordinate amount of time to reach steady state. Figure 7a clearly illustrates this concept, since only the case of extreme chatter (18mm) reached steady-state within the 15 revolutions that were simulated.

Case study 2: Multiple degree-of-freedom system

To further investigate the convergence and efficiency of the chatter criterion, a more complex milling scenario will now be considered, and the results compared to other chatter detection techniques. The system studied involved a tool with two modes of vibration in the x direction, and one in the y-direction. Full details of the simulation parameters are shown in Table 1. Three chatter criteria were investigated: the proposed self-excitation damping ratio, a non-dimensional chip thickness method [6], and a peak-to-peak forces method [5]. The self-excitation damping ratio method used the approach described above, with $\zeta=0$ defining the boundary of chatter stability. The non-dimensional chip

thickness method calculated the ratio η of the maximum chip thickness (during the simulation) to that which occurred with no structural dynamics. A threshold value of $\eta = 1.06$ was used to define the boundary of chatter stability. The peak-to-peak forces method measured the resultant of the vibration forces in the x and y directions and obtained the maximum peak-to-peak (PTP) value. Values of 200 and 400N were used as to define the boundary of chatter stability.

For each method, stability lobes were generated based upon simulations representing 5, 10, 20, and 50 revolutions of the tool. At each spindle speed, the depth of cut was determined that corresponded to the boundary of chatter stability, using a numerical search routine. The search routine was based upon the Matlab function *fzero* [15], which uses a combination of bisection, secant, and inverse quadratic interpolation [17]. However, it should be noted that the aim here was not to study the speed at which the stability boundary could be located, but rather how the location of the boundary (in terms of the depth of cut) was affected by the number of simulated tool revolutions.

Results for the self-excitation damping ratio are shown in Figure 8a. It can be seen that up to 10,000 rpm, the predicted stability boundary is approximately the same regardless of the number of simulated tool revolutions. For 5 revolutions the prediction is slightly more erratic, so in this region the solution can be said to have converged for 10 simulated tool revolutions. For the 'non-dimensional chip thickness' method, the corresponding result is shown in Figure 8b. Here, the predicted stability boundary is strongly dependant upon the number of simulated revolutions, throughout the spindle speed range. There is still a noticeable difference in the prediction between 20 and 50 simulated revolutions, although these results do appear to be converging. Again, the rate of convergence is markedly worse above 10,000 rpm. Figure 8c repeats this result for the peak-to-peak forces method. A comprehensive PTP forces diagram would require contour lines at a range of PTP forces. For clarity, Figure 8c shows the convergence of the 400N PTP contour as the number of simulated revolutions is increased, along with the 200N contour based upon 50 simulated revolutions. The convergence of this criterion appears to be worse than the non-dimensional chip thickness method, particularly at low spindle speeds.

To recap, Figure 8 demonstrates that at low spindle speeds the damping ratio method is clearly superior to the other methods in terms of the length of simulation that is required. However, the degradation in its performance at higher spindle speeds is worthy of further investigation. Analysis of the analytical chatter prediction suggests that the lobes above 10,000 rpm represent self-excited vibrations with less than one complete oscillation per tooth on the tool. This agrees with the Fourier analysis performed during the damping ratio calculation, which indicated that the self-excited spectral index k_p with the lowest damping ratio was less than 5. Dividing this by the number of teeth (four) shows that there is one or less complete self-excited oscillation per tooth pass. Consequently, the vibrations will not necessarily grow with every cycle of the tooth. This is illustrated in Figure 9a which plots the self-excitation vibration amplitude for different depths of cut. In the first 20 revolutions the self-excited vibration magnitude fluctuates with each analysis frame. Near the boundary of stability the vibrations tend to decay at first, but then grow in an unstable fashion, with a boundary of stability of 5mm. Figure 9b shows similar behaviour is observed in the chip thickness data: the oscillations appear to stabilise after 20 cycles, but in fact an unstable oscillation then begins to grow. This suggests that determining the chatter stability when there is less than one self-excited vibration per tooth pass will always require a large number of simulation cycles.

Case study 3: Stability and sensitivity

In the previous section, the self-excitation damping ratio was used to define the boundary of chatter stability, where the damping ratio is zero. However, this approach does not use all the information that is available, since the value of the damping ratio away from the boundary of stability offers additional insight into the behaviour. To illustrate this point, milling simulations (using the parameters shown in Table 1) were performed over a test matrix of spindle speeds from 3000 to 6000 rpm in steps of 20rpm, and depths of cut from 1mm to 10mm in 1mm steps. The data from each simulation was then analysed to calculate the self-excitation damping ratio. This data could then be presented graphically, as contour lines representing constant values of damping ratio for different spindle speeds and depths of cut.

The results are shown in Figure 10a, for contour lines of ζ=-0.002 (unstable cutting) ζ=0 (the chatter stability boundary) and ζ=0.002 (stable cutting). Compared to stability lobes obtained by other means, this graph yields more detailed information about the chatter stability. For example, at some spindle speeds (e.g. 4500rpm), the damping ratio is very insensitive to the depth of cut: large changes in the depth of cut result in only small variations in damping ratio. In other conditions (e.g. 5600 rpm), the damping ratio changes markedly as the depth of cut is increased. These two examples are illustrated in more detail in Figure 10b, which shows the variation in damping ratio for depths of cut between 2 and 10mm at 4500rpm compared to 5600rpm. This information is of practical benefit: At first sight, cuts of 3mm would appear to be 'equally stable' – the critical depth of cut being about 5mm – for both speeds. However, at 4500rpm the damping ratio is only 1/3 of that at 5600 rpm so the two situations are not 'equally stable'; a more conservative condition being 5600 rpm.

The sensitivity analysis that is made possible by the damping ratio method is thus well illustrated by Figure 10a and b. However, another advantage which comes to light is the linearity of the relationship between damping ratio and depth of cut. The linear region on Figure 10b extends from low depths of cut (where the low amplitude of the self-excited vibration can lead to numerical rounding errors), to high depths of cut. In severe chatter, the nonlinearity of the system causes the self-excited vibration to reach steady state (as was seen in Figure 7). As a consequence, a straight line fit will have a reducing gradient as the depth of cut (and hence the proportion of signal that is in steady state) increases. This is observed in Figure 10b for depths of cut above 9mm. Within the linear region, the smoothness of the damping ratio/depth of cut relationship makes it possible to search for the stability boundary (ζ=0) with efficient numerical routines that use interpolation techniques [18]. In contrast, other chatter criteria tend to be discontinuous at the boundary of stability, as is shown in Figure 10c (for the chip-thickness based criterion [6]), Figure 10d (for the PTP forces criterion [5]), and Figure 10e ('Variance' criterion [8]). This means that numerical search routines cannot effectively use the *value* of the chatter criteria to search for the chatter boundary, and so less efficient numerical methods (e.g. the bisection method [18]) must be used.

Case study 4: Low radial immersion cutting

As a final example to demonstrate the proposed stability criterion, the case of low radial immersion cutting is investigated. Cutting conditions (Table 1) were chosen that were identical to those used by Bayly *et al* [8], except that only a single mode of vibration was assumed. Figure 11a shows the stability lobes for a small region of spindle speeds. This region corresponds to self-excited vibration with between one and two oscillations per tooth. In this area, Bayly [8] showed that an additional region of stability exists due to the intermittent nature of the cutting process. The result in Figure 11a agrees with these findings. This used a simulation with 15 revolutions of the tool, along with the numerical optimisation method mentioned in Case study 2. Typically, between 4 and 10 simulation iterations were required at each spindle speed to locate the stability boundary. In contrast, the variance method [8] required a minimum of 40 revolutions and used an exhaustive search with 100 simulations for each spindle speed. However, the non-dimensional chip thickness criterion (also shown on Figure 11a), appears to converge more quickly at low radial immersions, needing just 20 revolutions to obtain the same result as the damping ratio method.

In Figure 11b, the nature of the self-excited oscillations is explored in the stable region resulting from interrupted cutting (18500rpm). It can be seen here that the self-excited vibrations tend to grow and decay in a periodic fashion, as if the signal possessed a 'beating' component. This can be explained by the intermittency of the cutting process: when the tooth is immersed in the cut, the vibrations are unstable and grow, whereas when the tooth is not immersed the vibrations exhibit free decay. Despite this periodic behaviour, the overall trend is similar to that for non-intermittent cutting. Figure 11c shows that outside the region of intermittent cutting stability, the self-excited vibrations behave the same as for high radial immersion cutting.

Discussion

The numerical examples described above have served to demonstrate the performance of the proposed chatter criterion under various conditions. At this stage, a number of issues are worthy of additional discussion. First, it should be noted that the present study has relied purely on numerical results. However, the modelling approach that has been used is adapted directly from the work of others [6],

and the results agreed very closely with the corresponding commercial software [13]. Any differences in the model predictions can be attributed to the simplifications of the model used in the present study, and the differences in the numerical solution/integration methods.

The proposed chatter criterion does impose some restrictions on the numerical methods used to solve the model. Most importantly, the number of simulation time steps per revolution of the tool (N) must be an integer value. This ensures that the periodic vibrations lie on the spectral lines of the Discrete Fourier Transform (DFT), so that they can be isolated from the self-excited vibrations. The value of N also impinges upon the efficiency of the signal processing analysis, since faster DFT algorithms can be used for data sequences with low prime factors [19]. Consequently, the chatter criterion cannot always be used immediately with existing time-domain models, since some modifications to the solution method may be necessary.

A related issue concerns the applicability of the method to milling tools with irregular teeth, where the teeth are not distributed evenly around the tool's circumference. In this case, the forced vibrations (at harmonics of the tooth passing frequencies) are not integer multiples of the tool rotation frequency. This makes it impossible to isolate the forced vibrations from the self-excited vibrations using the methods described in the present article. Consequently, further work is needed to investigate whether the proposed chatter criterion can be adapted for this special category of milling simulation.

Two other cutting scenarios have not been considered in the present study: tools with a single tooth, and helical tools. Tools with a single tooth are unusual because the tooth passing frequency is the same as the tool rotation frequency. Consequently, if only one tool rotation is used for each analysis frame, then (from (4)) the forced vibrations will manifest themselves in every spectral frequency of the DFT. This can be avoided by simply using two tool revolutions for each analysis frame, thereby doubling the spectral resolution. Helical tools have not been considered here because simulations of tools with a zero helix angle are considerably faster. Due to the axial symmetry only a single axial slice of the cutting kinematics need be considered. Some similar results have been obtained for a helical tool, but owing to the computational requirements they are less complete, and have not been included here for the sake of brevity.

A final issue that is worth considering is the possibility of applying the technique to experimental cutting tests. Compared to established spectral analysis methods (e.g. using audio measurements [10]), the analysis would require a much shorter sequence of data and yield additional physical insight. However, for stable cutting the measurement would have to include the initial disturbance to the system (when cutting first begins) so as to observe the decay in the self-excited vibration. Also, data sampling rates at an exact multiple of the spindle rotation would probably be impossible, so additional signal processing may be required.

Conclusions

In this article, a new method for analysing the chatter stability of time-domain milling simulations has been proposed. The method relies on signal processing of the predicted vibrations of the tool and workpiece, to calculate the so-called self-excitation damping ratio. Currently the method is only appropriate for tools with regular pitch teeth, and further work is needed to adapt the signal processing approach for the case of variable-pitch tools.

Compared to existing chatter criteria, the method has the following advantages:

1) The chatter stability can be predicted after substantially shorter runs of the simulation. Consequently, the speed of the chatter prediction is often at least five times faster.

2) The analysis yields more detailed information concerning the stability of the system. The chatter stability criterion is in fact a special case where the self excitation damping ratio equals zero, and non zero damping ratios can be used to give information on the relative stability of the system under different conditions. In addition, the analysis indicates the frequency and axis of motion of the self-excited vibrations.

3) The self-excitation damping ratio tends to change smoothly and continuously as the depth of cut is changed. Consequently, the boundary of chatter stability can be searched for using efficient numerical routines that base their iterative search upon the value of the damping ratio.

4) The signal processing approach provides more information on the behaviour of the self-excited vibrations. For stable milling they are often seen to decay in a linear fashion, whereas when

chatter occurs the onset of limit-cycle behaviour is observed due to the nonlinearity of the cutting process. For low radial immersion cutting, additional regions of stability can be observed under certain operating conditions, and in this case the self-excited vibrations include an additional periodic component.

Further work will investigate the application of the technique to experimental, rather than simulated, data, and consider the case of variable pitch tool geometry.
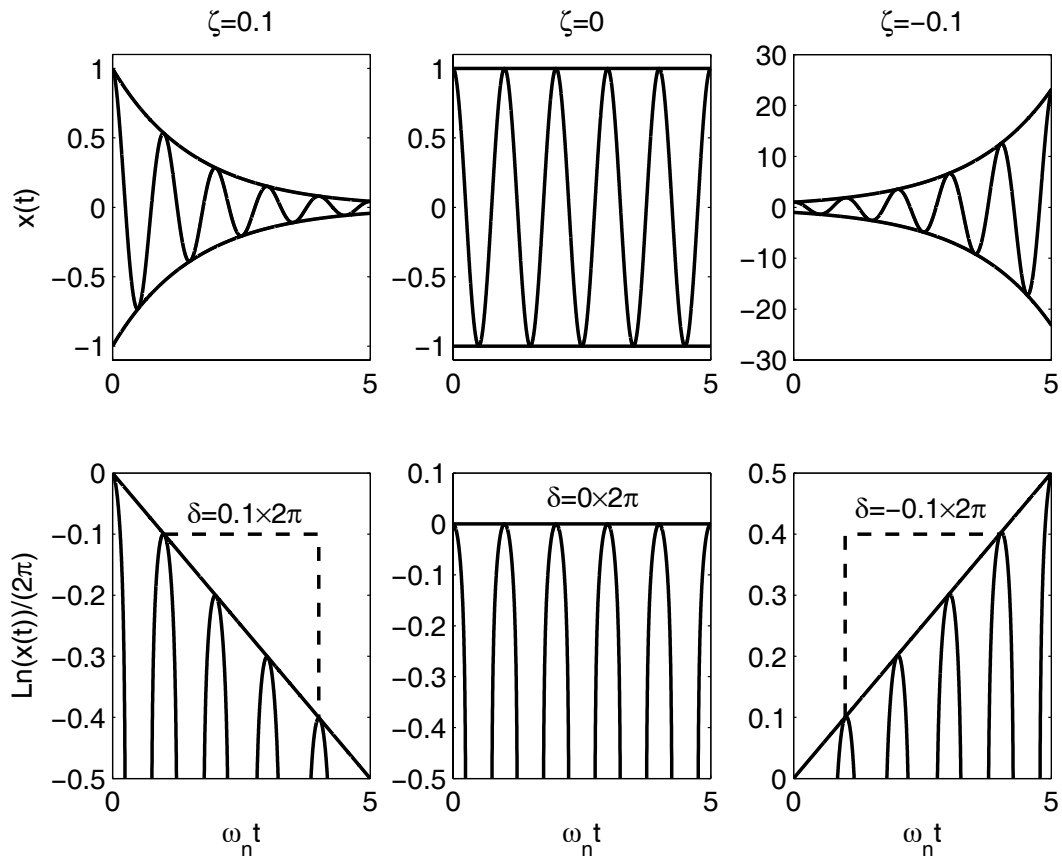
Acknowledgements

| Case study 1	
Tool diameter	20mm
Number of teeth	4
Flute helix	0° (axial flutes)
Milling mode	Up-milling
Spindle speed	3000 rpm
Radial immersion	8mm
Feed per tooth	0.05mm
y-direction mode 1: frequency damping: stiffness	700Hz 0.3% 80MN/m
K_{tc}	796.1 N/mm^2 (Al7075-T6 [13])
K_{rc}	168.8 N/mm^2 (Al7075-T6 [13])
Iterations per revolution:	256
Case studies 2 and 3	
Tool diameter	20mm
Number of teeth	4
Flute helix	0° (axial flutes)
Milling mode	Up-milling
Radial immersion	8mm
Feed per tooth	0.05mm
x-direction mode 1: frequency damping: stiffness	600Hz 1% 70MN/m
x-direction mode 2: frequency damping: stiffness	900Hz 1% 50MN/m
y-direction mode 1: frequency damping: stiffness	700Hz 0.3% 80MN/m
K_{tc}	796.1 N/mm^2 (Al7075-T6 [13])
K_{rc}	168.8 N/mm^2 (Al7075-T6 [13])
Iterations per revolution:	256
Case study 4	
Tool diameter	12.7mm
Number of teeth	2
Flute helix	0° (axial flutes)
Milling mode	Up-milling
Radial immersion	5%
Feed per tooth	0.05mm
x-direction mode 1: frequency damping: stiffness	922Hz 1.1% 1.34MN/m
K_{tc}	600 N/mm^2 (source: [8])
K_{rc}	200 N/mm^2 (source: [8])
Iterations per revolution:	256

**Table 1: Parameters for the case studies**

List of Figures

Figure 1: Free vibrations of a linear, viscously damped system with positive (ζ=0.1), zero (ζ=0), and negative (ζ=-0.1) damping, corresponding to stable, marginally stable, and unstable self-excited vibration systems.
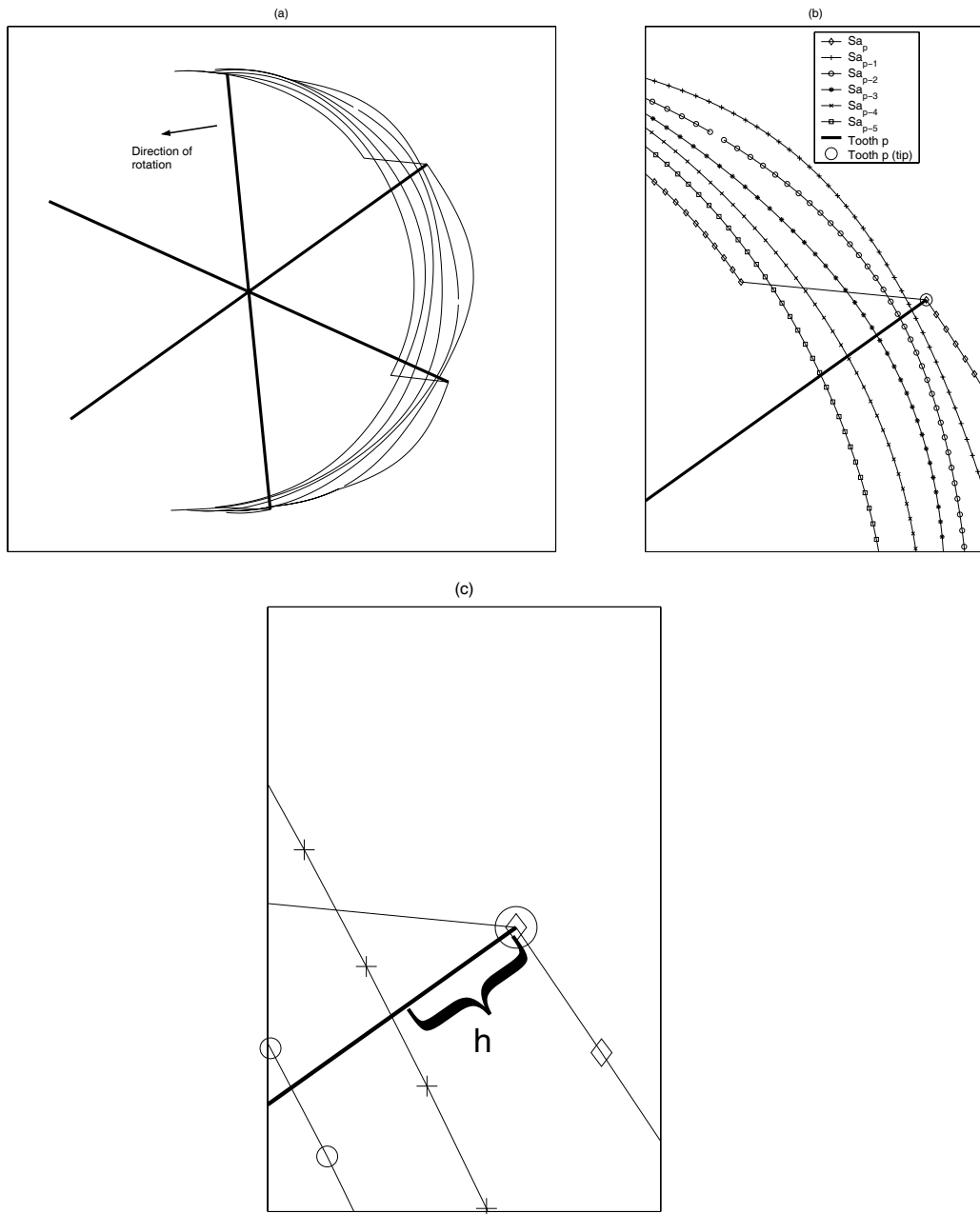
Figure 2: Chip thickness calculation
(a) 6-toothed tool, with an array of discrete surface points for each tooth.
(b) Close up of one tooth, showing updating of the surface points.
(c) Calculation of the chip thickness h.
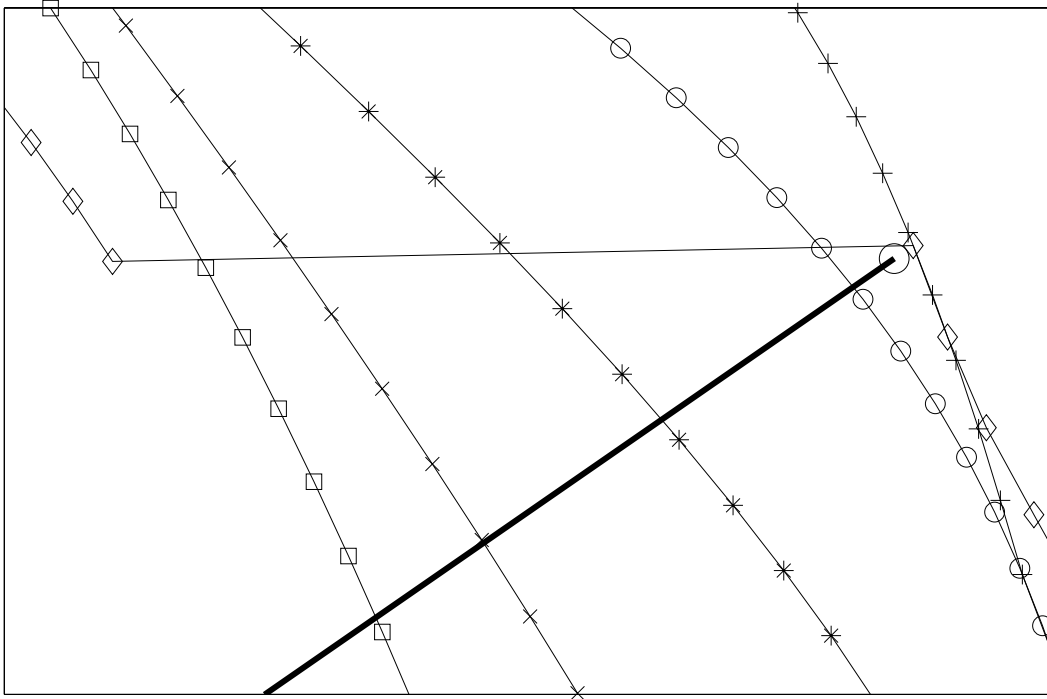
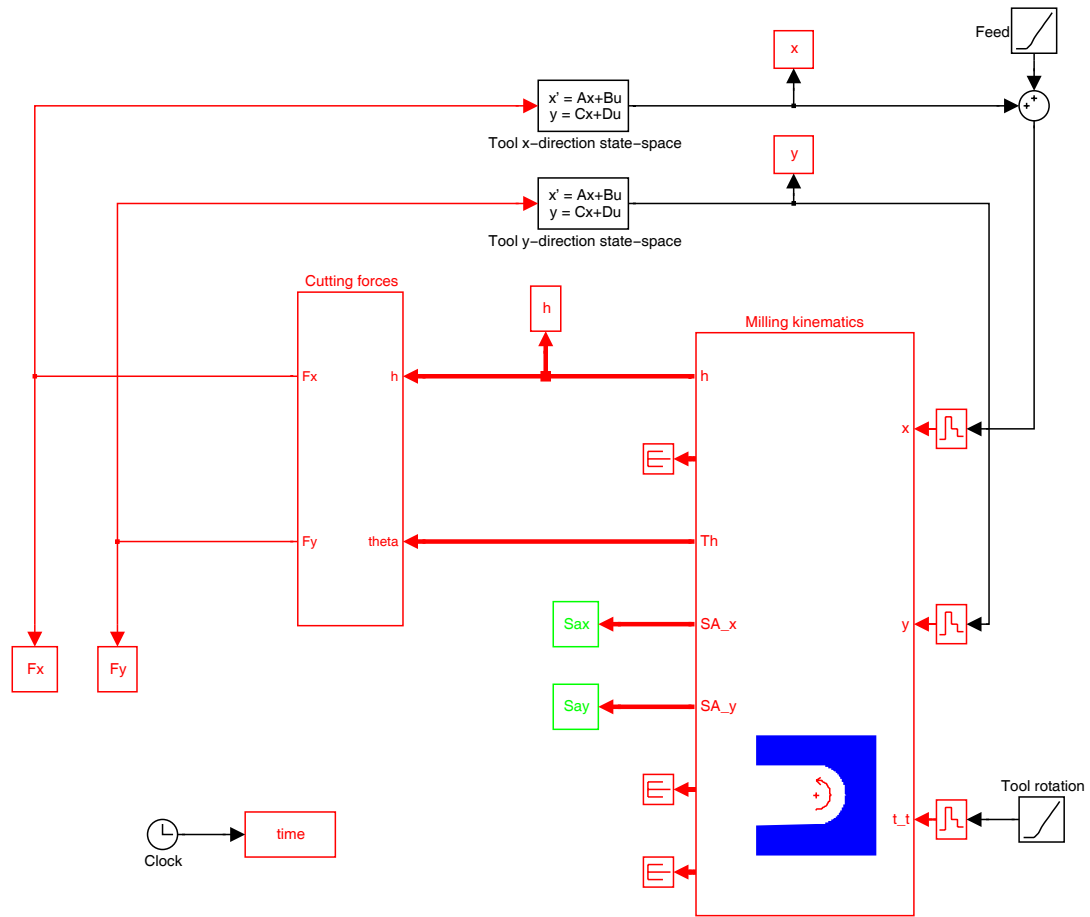**Figure 3: Updating the surface points when the tooth is not engaged in the cut**

Figure 4: Simulink block diagram of the milling simulation

```
┌─────────────────────┐          ┌──────────────────────────┐
│          A          │          │  Simulation parameters   │
│     Time domain     │ ◄─────── │      Depth of cut        │
│     simulation      │          │     Spindle speed        │
└─────────────────────┘          │      Cut geometry        │
                                 │      Tool geometry       │
                                 │   Simulation settings    │
                                 └──────────────────────────┘

┌─────────────────────┐
│  For each degree of │ ◄──────────────────────────────┐
│  freedom of the     │                                 │
│  system:            │                                 │
└─────────────────────┘                                 │

┌─────────────────────┐          ┌──────────────────────────┐
│         B:          │          │           E:             │
│  Divide signal into │          │  Find spectral lines kp  │
│  F frames each of   │          │  which have maximum      │
│  length N,          │          │  values                  │
│  representing 1     │          └──────────────────────────┘
│  tool cycle         │
│  x(n,F)             │          ┌──────────────────────────┐
└─────────────────────┘          │           F:             │
                                 │  Take logarithms to show │
┌─────────────────────┐          │  the self-excited        │
│         C:          │          │  vibration decay per     │
│  Take the discrete  │          │  cycle (i.e. frame)      │
│  Fourier transform  │          └──────────────────────────┘
│  X(k,F)             │
│                     │          ┌──────────────────────────┐
└─────────────────────┘          │           G:             │
                                 │  Fit a 1st order         │
┌─────────────────────┐          │  polynomial and select   │
│         D:          │          │  the spectral line       │
│  Set tooth passing  │          │  kp,max with the         │
│  frequency          │          │  steepest gradient       │
│  harmonics to zero  │          └──────────────────────────┘
│  Xse(m+nt,F)=0,     │
│  m=1,2,3,4,…        │    ┌──────────────────────────┐   ┌──────┐
└─────────────────────┘    │ ζ=δR,kpmax/(2πkp,max)    │ ► │  ζ   │
                           └──────────────────────────┘   └──────┘
```

A

Time domain simulation

Simulation parameters
Depth of cut
Spindle speed
Cut geometry
Tool geometry
Simulation settings

For each degree of freedom of the system:

B:
Divide signal into F frames each of length N, representing 1 tool cycle
$x(n,F)$

C:
Take the discrete Fourier transform
$X(k,F)$

D:
Set tooth passing frequency harmonics to zero
$X_{se}(m+n_t,F)=0$,
$m=1,2,3,4,…$

E:
Find spectral lines k_p which have maximum values

F:
Take logarithms to show the self-excited vibration decay per cycle (i.e. frame)

G:
Fit a 1st order polynomial and select the spectral line $k_{p,max}$ with the steepest gradient
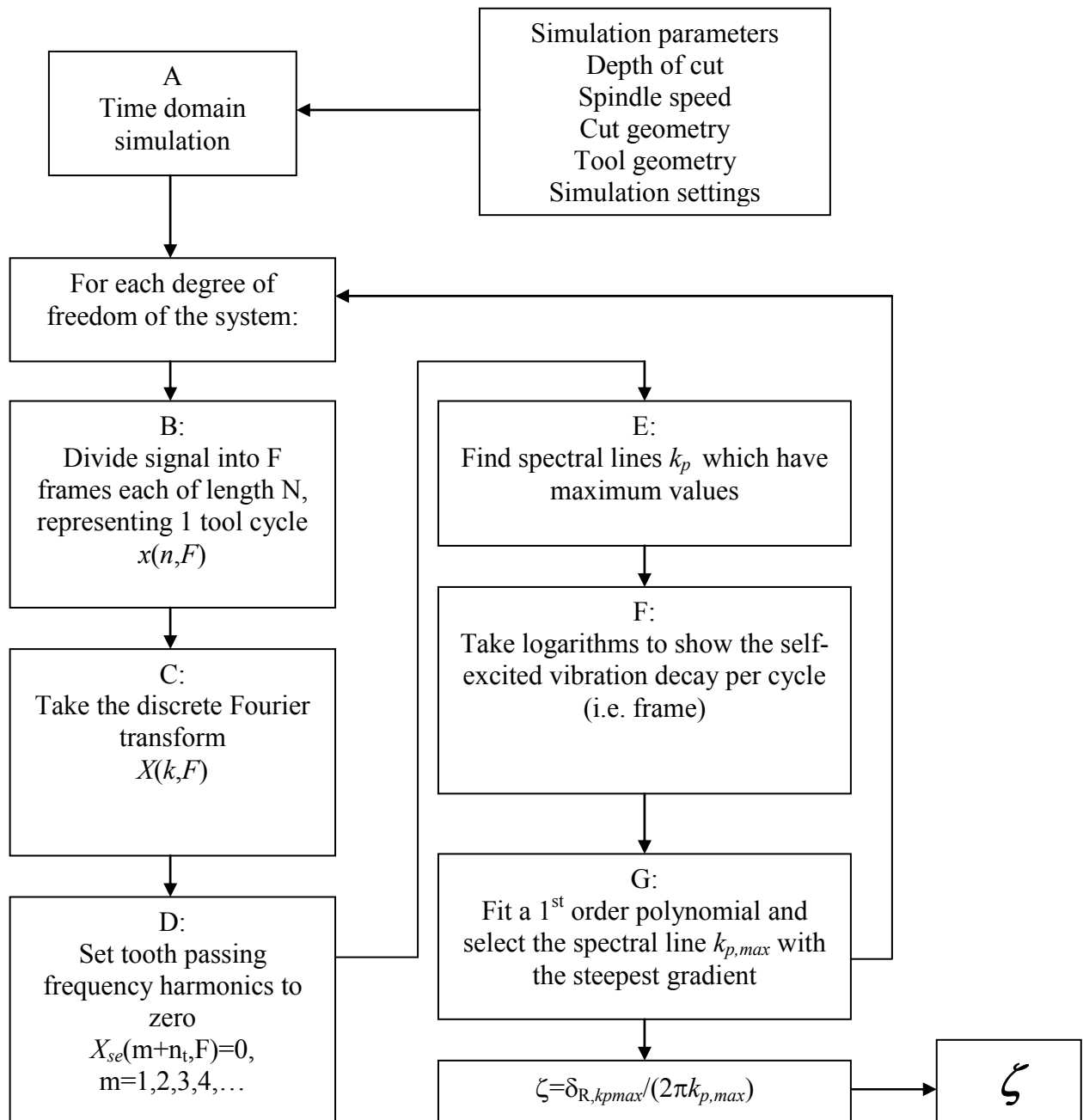
$\zeta=\delta_{R,kpmax}/(2\pi k_{p,max})$
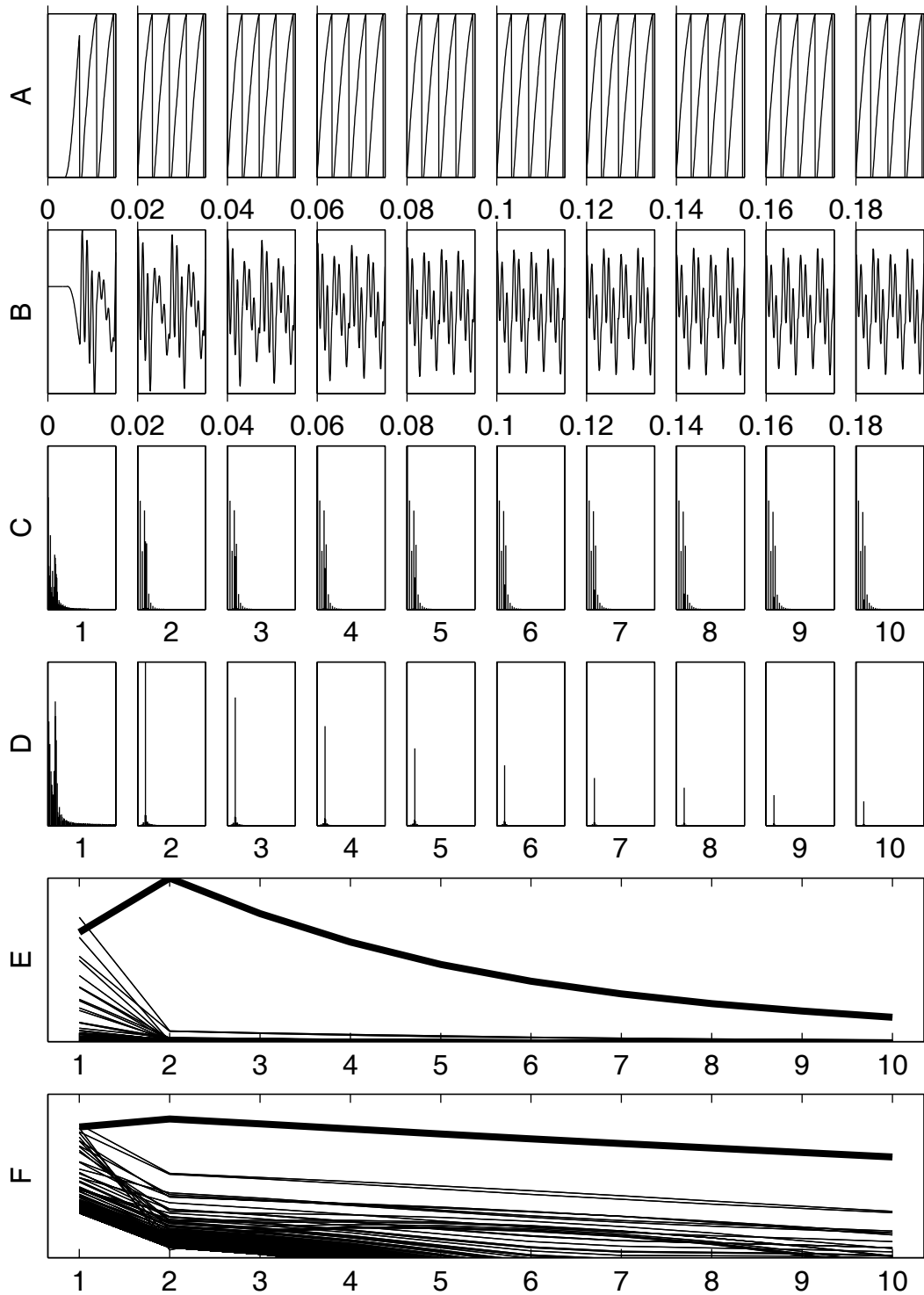
ζ

Figure 5: Flow chart to illustrate evaluation of the chatter criterion, ζ.

Figure 6: Example of chatter detection for a stable cut.
(A) Chip thickness against time, divided into 10 frames
(B) Y-direction vibration against time, divided into 10 frames
(C) Discrete Fourier Transform (DFT) of (B)
(D) DFT with tooth-passing frequency harmonics removed
(E) Data in (D) plotted against frame number
(F) logarithm of the useful data in (E)

(a)

(b)
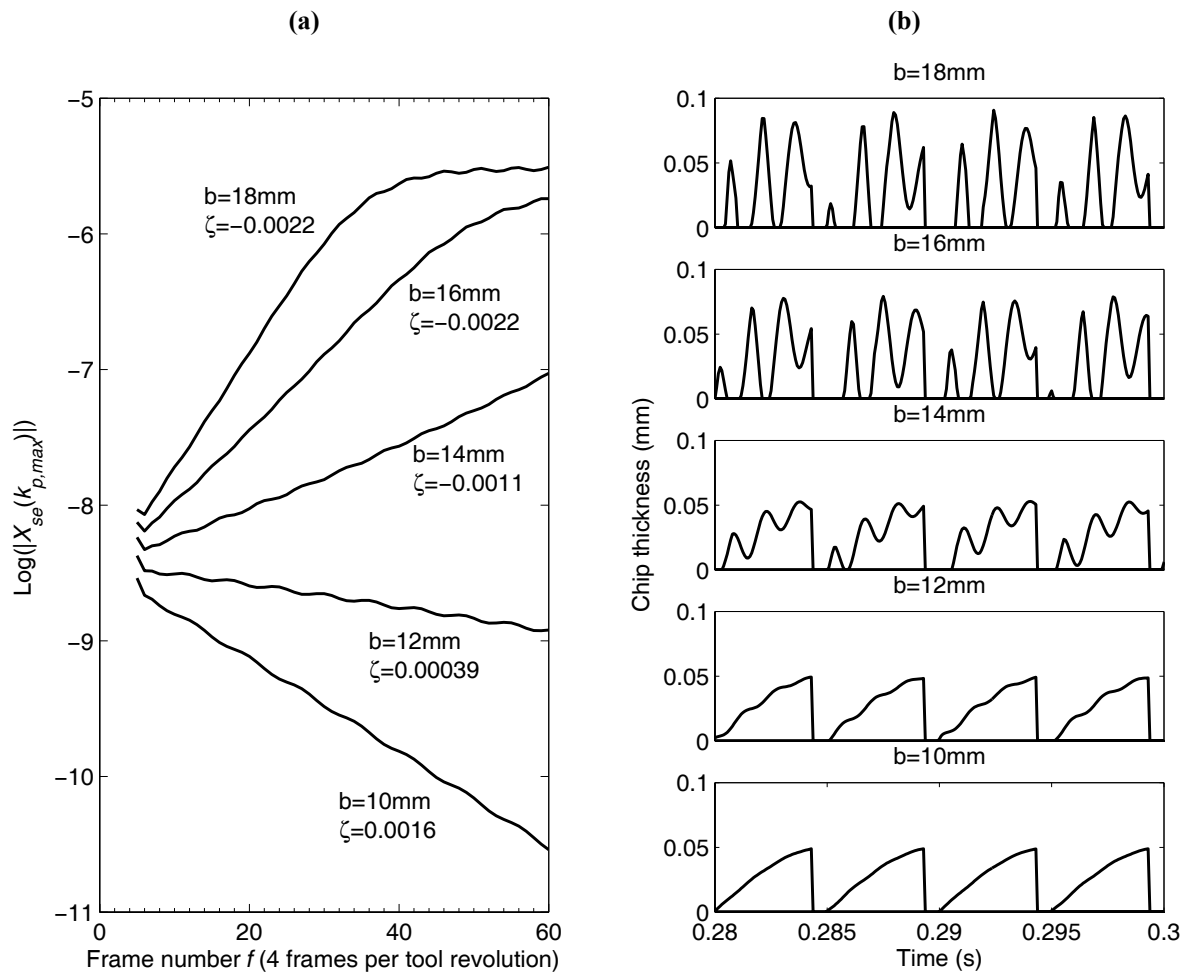
Figure 7: Effect of the depth of cut on
(a) the stability criterion ζ and self-excited vibration magnitude
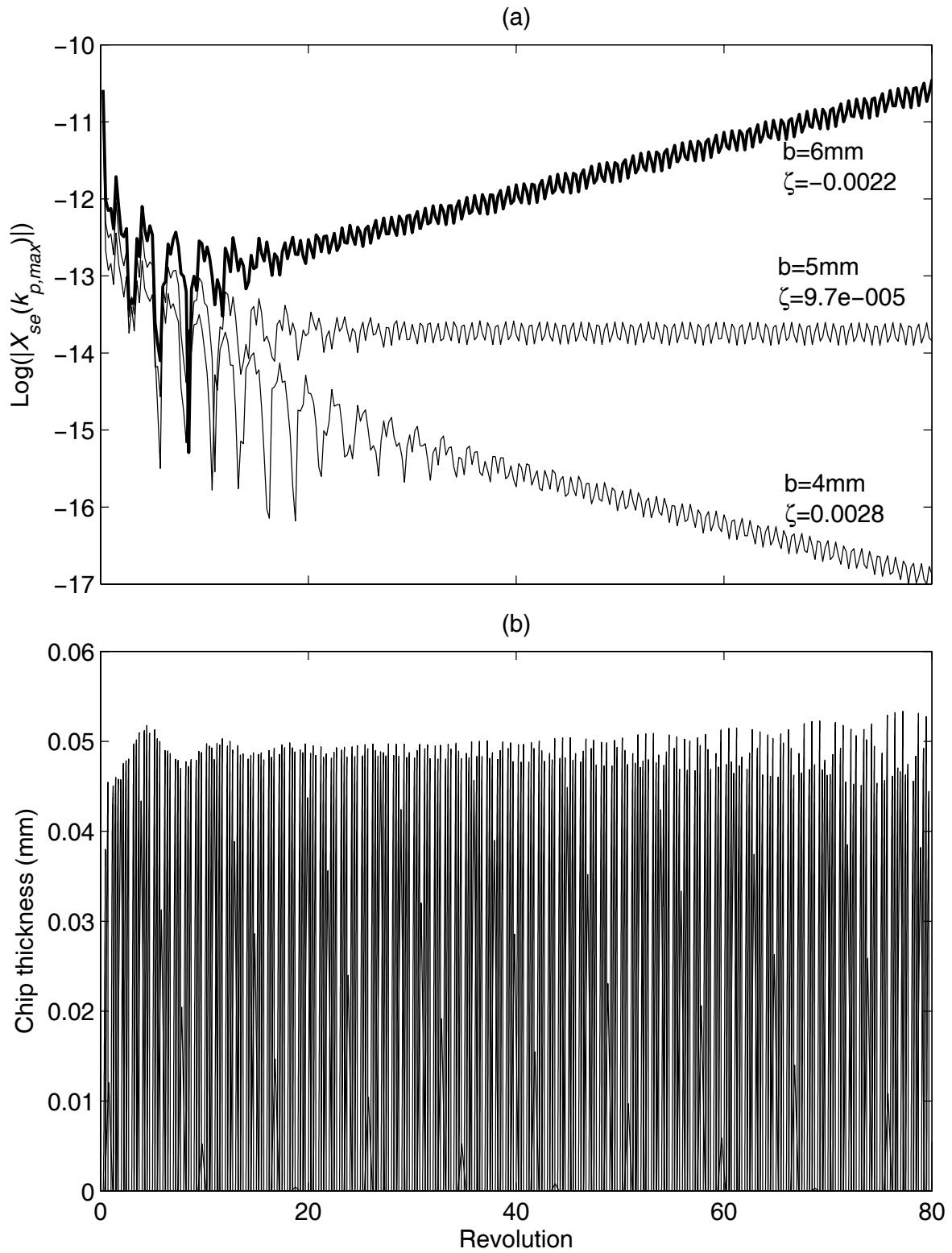**(b) Chip thickness in the last tool revolution**

(a)

(b) **(c)**
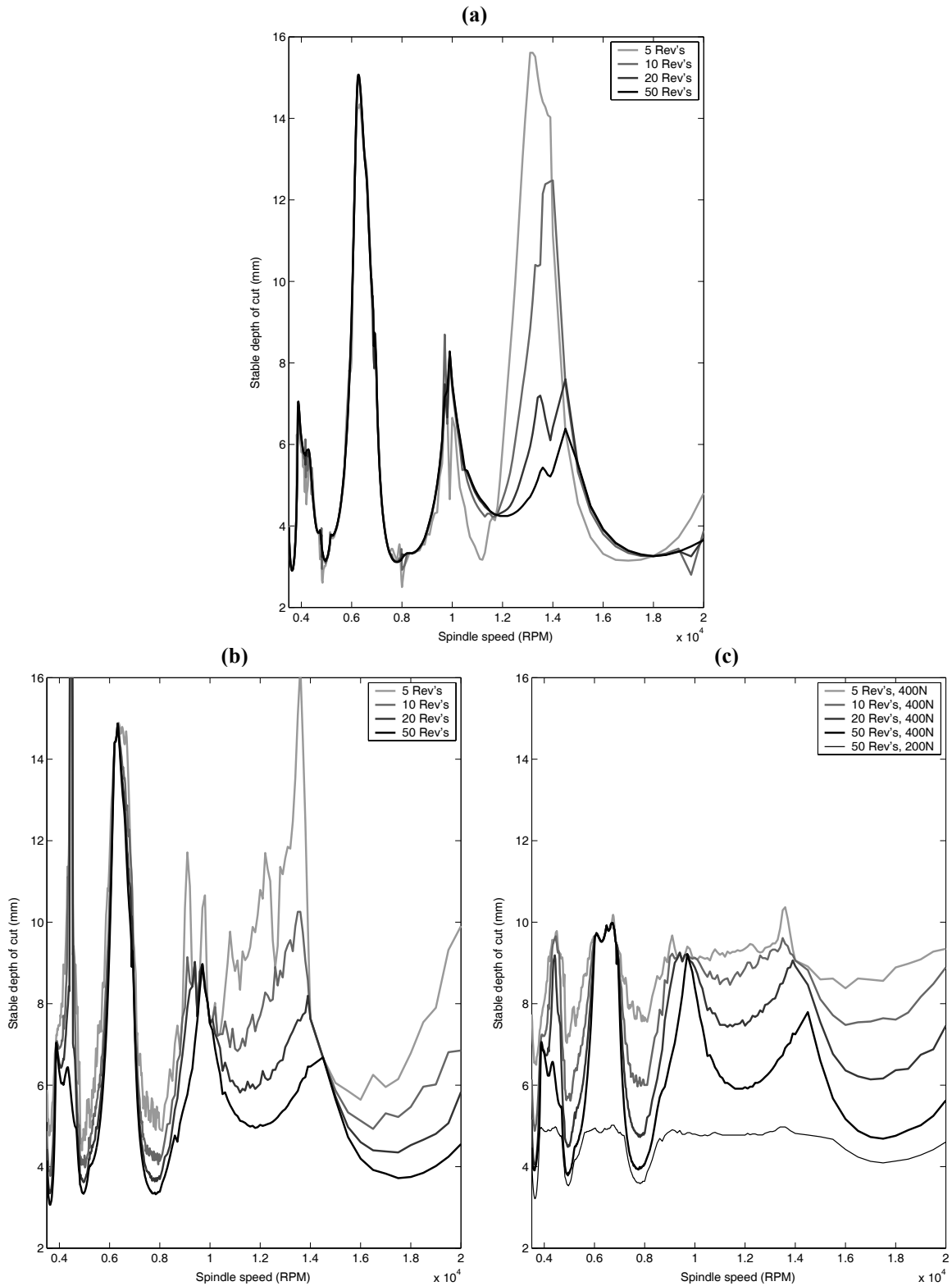
Figure 8: Convergence of stability lobes as the simulated number of tool revolutions increases
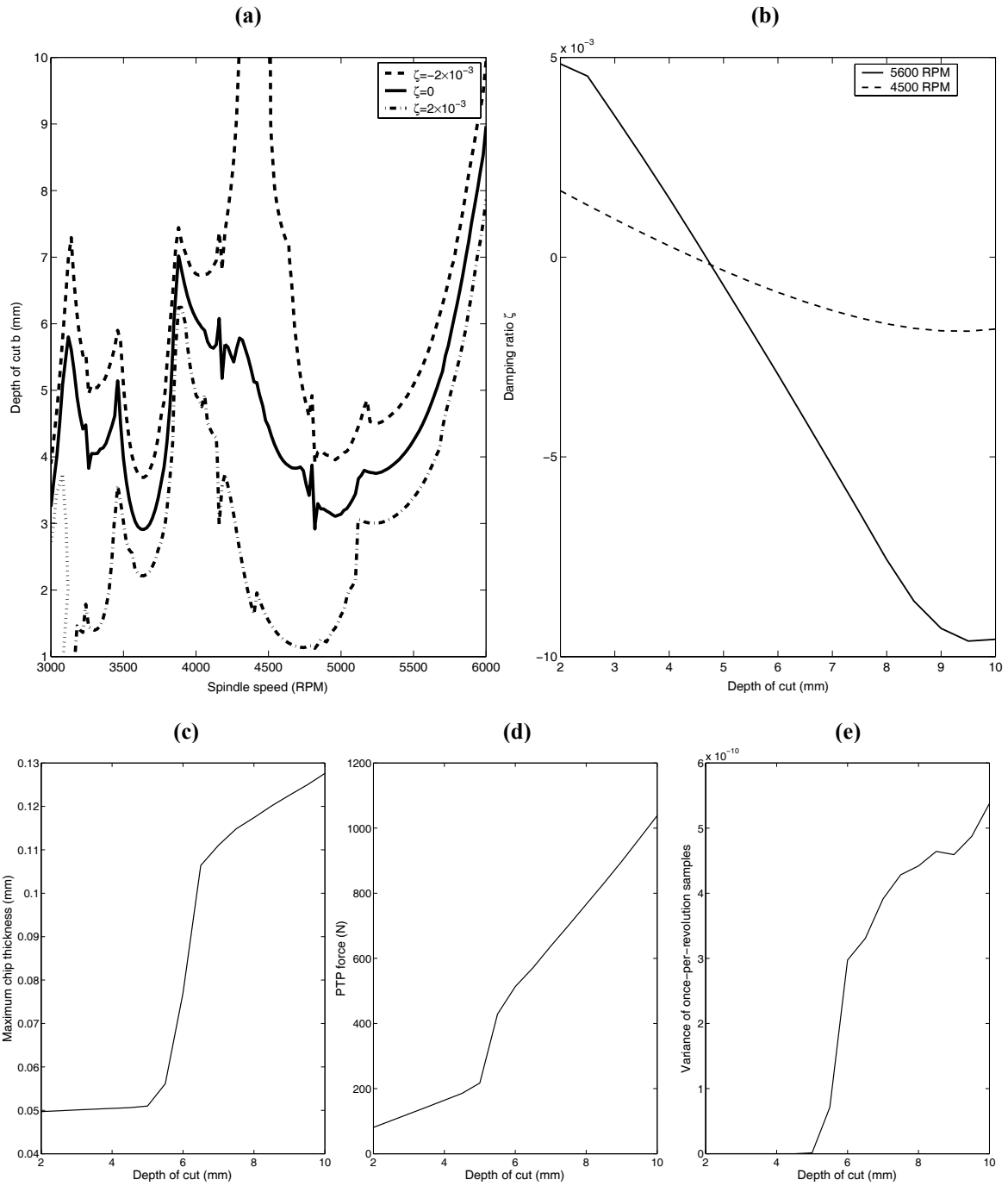**(a) Self-excitation damping ratio (ζ=0) stability criterion**
(b) 'non-dimensional chip thickness ' stability criterion [6]
**(c) 'peak-to-peak forces' stability criterion [5]**

Figure 9: Convergence at 14000rpm.
(a) Self-excitation vibrations for 200 tool revolutions
(b) Chip thickness for first 100 revolutions at 6mm depth of cut

Figure 10: Damping and sensitivity analysis.
(a) Stability lobes with predictions of system damping
(b) Damping ratio at 4500rpm and 5600rpm
(c) Maximum chip thickness (5600rpm)
(d) PTP forces (5600rpm)
(e) Variance of once-per revolution samples (5600 rpm)
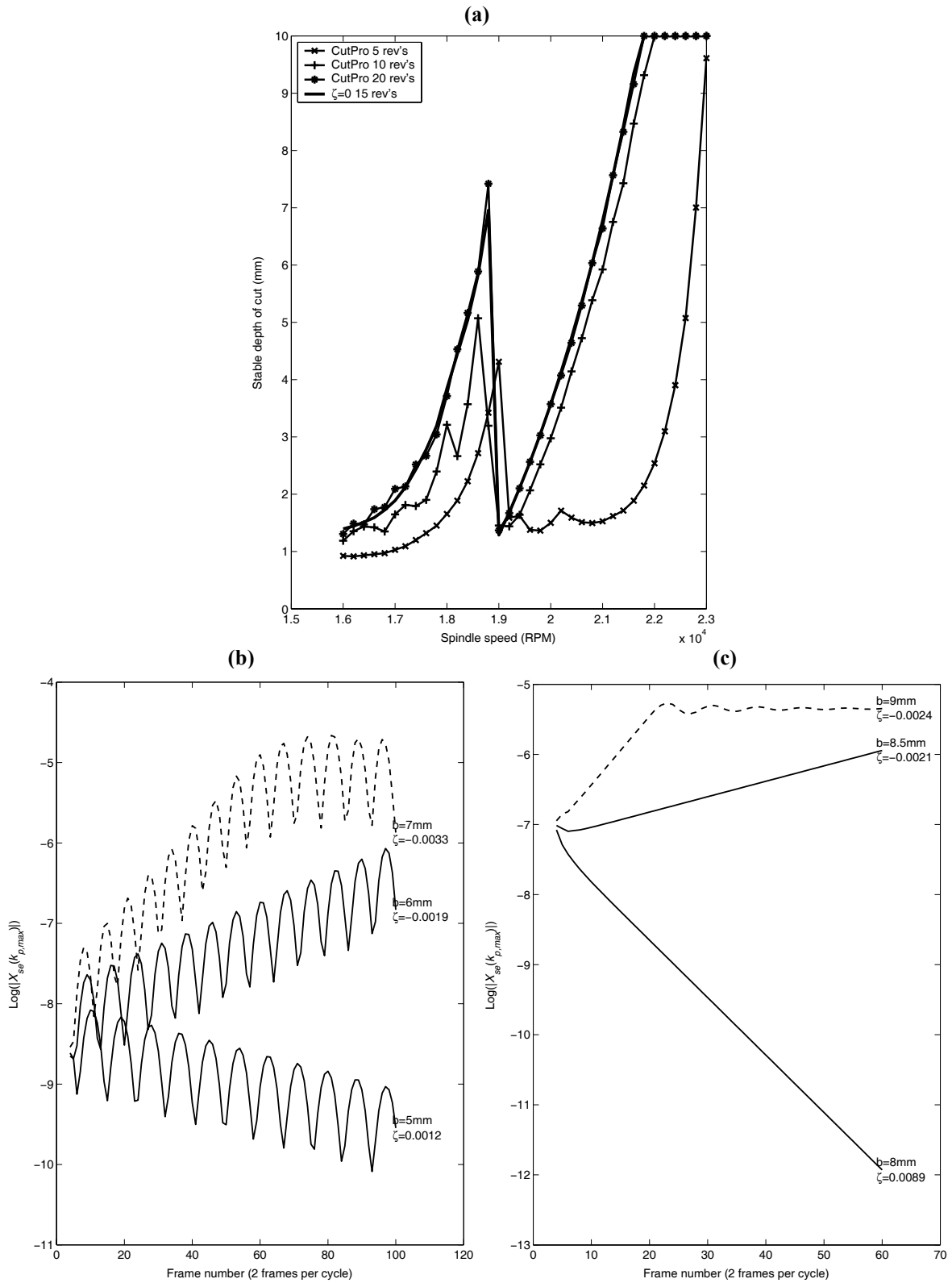
Figure 11: Low radial immersion cutting.
(a) Stability lobes using 'non-dimensional chip thickness' method (η) and damping ratio method (ζ)
(b) Self-excited vibrations at 18,500rpm (c) Self-excited vibrations at 21,400 rpm.

References

1. Tlusty, J. and Polacek, M., 1963, "The stability of the machine tool against self excited vibration in machining," *ASME Proceedings of the Engineering Research Conference*, pp. 465-454.

2. Tobias, S. A. and Fishwick, W., 1958, "Theory of Regenerative Machine Tool Chatter," *The Engineer*, pp. 199-203.

3. Smith, S. and Tlusty, J., 1991, "An Overview of Modeling and Simulation of the Milling Process," *Journal of Engineering for Industry*, **113**, pp. pp.169-175.

4. Altintas, Y. and Budak, E., 1995, "Analytical prediction of stability lobes in milling," *CIRP Annals*, **44**, pp. 357-362.

5. Smith, S. and Tlusty, J., 1990, "Update on High-Speed Milling Dynamics," *Journal of Engineering for Industry*, **112**, pp. 142-149.

6. Campomanes, M. L. and Altintas, Y., 2003, "An improved time domain simulation for dynamic milling at small radial immersions," *Journal of Manufacturing Science and Engineering*, **125**, pp. 416-422.

7. Li, H. Z., X.P., K., and X.Q., C., 2003, "A novel chatter stability criterion for the modelling and simulation of the dynamic milling process in the time domain," *International Journal of Advanced Manufacturing Technology*, **22**, pp. 619-625.

8. Bayly, P. V., Mann, B. P., Schmitz, T. L., Peters, D. A., Stepan, G., and Insperger, T., 2002, "Effects of radial immersion and cutting direction on chatter stability in end milling," *ASME International Congress and Exposition*, **13**, pp. 351-363.

9. Schmitz, T. L., Medicus, K., and Dutterer, B., 2002, "Exploring once-per-revolution audio signal variance as a chatter indicator," *Machining Science and Technology*, **6** (2), pp. 215-233.

10. Delio, T., Tlusty, J., and Smith, S., 1992, "Use of audio signals for chatter detection and control," *Journal of Engineering for Industry*, **114** (2), pp. 146-157.

11. Rao, S. S., 2004, *Mechanical Vibrations*. Pearson Prentice Hall.

12. Tlusty, J., 1999, *Manufacturing Processes and Equipment*. Prentice Hall, New Jersey.

13. CutPro, 2004. Manufacturing Automation Laboratories, Inc, Vancouver.

14. MetalMax MilSim, 2004. Manufacturing Laboratories, Inc, Las Vegas.

15. Matlab, 2004. The Mathworks, Inc, Natick.

16. Kondo, E., Ota, H., and Kawai, T., 1997, "New method to detect regenerative chatter using spectral analysis, Part 1: basic study on criteria for detection of chatter," *Journal of Manufacturing Science and Engineering*, **119** (4(A)), pp. 461-466.

17. Forsythe, G. E., Malcolm, M. A., and Moler, C. B., 1976, *Computer Methods for Mathematical Computations,*. Prentice-Hall.

18. Atkinson, L. V., Harley, P. J., and Hudson, J. D., 1989, *Numerical Methods with fortran 77.* Addison Wesley, England.

19. Frigo, M. and Johnson, S. G., 1998, "FFTW: An adaptive software architecture for the FFT," *Proceedings of the International Conference on Acoustics, Speech, and Signal Processing*, **3**, pp. 1381-1384.